

Hole doping by pressure on the 1111 pnictides CaFeAsF and SrFeAsF

This content has been downloaded from IOPscience. Please scroll down to see the full text.

2014 J. Phys.: Condens. Matter 26 155702

(<http://iopscience.iop.org/0953-8984/26/15/155702>)

View [the table of contents for this issue](#), or go to the [journal homepage](#) for more

Download details:

IP Address: 168.96.66.131

This content was downloaded on 16/06/2014 at 19:19

Please note that [terms and conditions apply](#).

Hole doping by pressure on the 1111 pnictides CaFeAsF and SrFeAsF

Daniele C Freitas¹, Gastón Garbarino², Ruben Weht^{3,4}, Amadou Sow¹, Xiyu Zhu⁵, Fei Han⁵, Peng Cheng⁵, Jing Ju⁵, Hai Hu Wen⁵ and Manuel Núñez-Regueiro¹

¹ Institut Néel, Centre National de la Recherche Scientifique (CNRS) & Université Joseph Fourier (UJF), 25 Avenue des Martyrs, BP166, F-38042 Grenoble Cedex 9, France

² European Synchrotron Radiation Facility (ESRF), 6 Rue Jules Horowitz, BP 220, 38043 Grenoble, France

³ Gerencia de Investigación y Aplicaciones, Comisión Nacional de Energía Atómica (CNEA), Avda. General Paz y Constituyentes, 1650-San Martín, Argentina

⁴ Instituto Sabato, Universidad Nacional de San Martín-CNEA, 1650-San Martín, Argentina

⁵ National Laboratory for Superconductivity, Institute of Physics and Beijing National Laboratory for Condensed Matter Physics, Chinese Academy of Sciences, PO Box 603, Beijing 100190, People's Republic of China

E-mail: manolo.nunez-regueiro@neel.cnrs.fr

Received 18 December 2013, revised 15 February 2014

Accepted for publication 25 February 2014

Published 27 March 2014

Abstract

We determine the pressure phase diagram of the 1111 compounds CaFeAsF and SrFeAsF, up to 20 GPa and down to 4 K by electrical resistivity measurements and the change of structure up to 40 GPa at room temperature. The antiferromagnetic transition temperature, as determined by the derivative peak, shows a minimum at ~5 GPa (10 GPa) for the Ca (Sr) compound. For CaFeAsF, superconductivity appears at this minimum, coincident with the development of a previously reported monoclinic phase. For SrFeAsF, where the orthorhombic and the monoclinic phase were reported to coexist, superconductivity exists above $P \geq 1$ GPa. Both phase diagrams can be scaled by a shift of ~10 GPa pressure at which the volume of SrFeAsF and that of CaFeAsF at ambient pressure coincide. The difference of our phase diagram with that of electron-doped 1111 samples is accounted for by hole doping under pressure, which we verified through electron band structure calculations.

Keywords: iron superconductors, phase diagram, pressure

(Some figures may appear in colour only in the online journal)

The first discovered iron superconductors [1] were the so-called 1111 phases that are composed of stacked LnO layers and FeAs layers (Ln is a lanthanide) in a tetragonal ($P4/nmm$) ZrCuSiAs-type structure. At temperatures around 150 K, depending on the lanthanide, an orthorhombic ($Cmma$) distortion develops, followed by an antiferromagnetic state several degrees Kelvin below [2]. The antiferromagnetic state is currently attributed to the development of a spin density wave (SDW), caused by the nesting of the cylindrical hole and electron sheets of the Fermi surface [3]. Electron doping by, for example, replacing oxygen with fluorine leads to the disappearance of both the orthorhombic distortion and the SDW [4], and the emergence of superconductivity. The

phase diagram of electron-doped 1111 compounds has been largely studied and it seems that there is almost no coexistence between the antiferromagnetic and superconducting phases, i.e. the transition as a function of doping is apparently of first order [5, 6, 7]. It has also been shown that hole doping of 1111 compounds can induce superconductivity [8, 9]. However, there is to date no detailed study of the hole-doped phase diagram of 1111 compounds. Such a study is of central importance, as in cuprates the phase diagram is different for holes and electrons, posing stringent restrictions on possible theories [10]. On the high temperature cuprate superconductors it is accepted that application of pressure is equivalent to hole doping [11]. Simply speaking, the positively charged

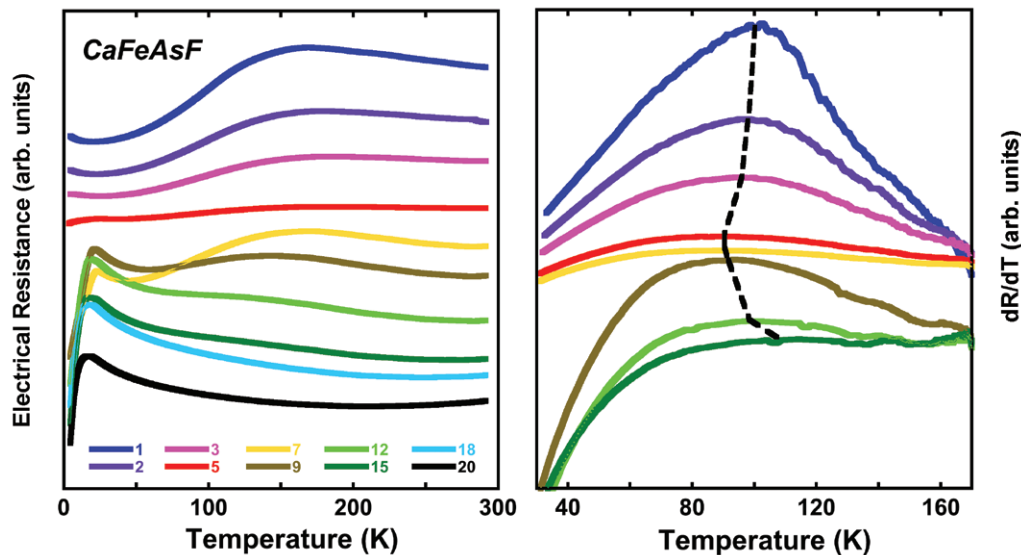


Figure 1. Left panel: example of the evolution with pressure of the temperature dependence of the electrical resistance of one sample of CaFeAsF. We observe the gradual appearance of superconductivity above 5 GPa. Right panel: the temperature derivative of the electrical resistance showing how we determine T_N , the transition temperature to the antiferromagnetic state. The dashed line marks its evolution with pressure; above 18 GPa there is no maximum in the curves for this sample. All other samples reported here showed a similar behavior.

reservoir layers pump electrons from the negatively CuO_2^{2-} layers as pressure reduces the distance that separates them. In analogy with cuprates, application of pressure has been shown to induce hole doping in the FeAs planes in the iron superconductor $\text{Sr}_{1-x}\text{K}_x\text{Fe}_2\text{As}_2$ [12]. Thus one way to study the hole-doped phase diagram would be to apply pressure and follow the different transition temperatures. We report here on coupled transport and structural studies, combined with electronic band structure calculations, of 1111 CaFeAsF and SrFeAsF under pressure.

The CaFeAsF (SrFeAsF) samples were prepared using a two-step solid-state reaction method, as used for preparing the LaFeAsO samples [13]. In the first step, CaAs (SrAs) was prepared by reacting Ca (Sr) flakes (purity 99.9%) and As grains (purity 99.99%) at 500 °C for 8 h and then 700 °C for 16 h. They were sealed in an evacuated quartz tube when reacting. Then the resultant precursors were thoroughly grounded together with Fe powder (purity 99.95%) and FeF_3 powder (purity 99%) in stoichiometry as given by the formula CaFeAsF (SrFeAsF). All the weighing and mixing procedures were performed in a glove box with a protective argon atmosphere. Then the mixture was pressed into pellets and sealed in a quartz tube with an argon atmosphere of 0.2 bar. The materials were heated up to 950 °C with a rate of 120 °C h⁻¹ and maintained for 60 h. Then a cooling procedure to room temperature was followed.

The electrical resistance measurements were performed using a Keithley 220 source and a Keithley 2182 nanovoltmeter. Pressure measurements, 1.4–22 GPa (between 4.2 and 300 K), were done in a sintered diamond Bridgman anvil apparatus using a pyrophyllite gasket and two steatite disks as the pressure medium [14]. Pressure cannot be cycled and thus measurements are done only with increasing pressure.

The angle dispersive x-ray diffraction studies on CaFeAsF and SrFeAsF powder samples were performed at the ID27

high-pressure beamline of the European Synchrotron Radiation Facility using monochromatic radiation ($\lambda = 0.3738 \text{ \AA}$) and diamond anvil cells. The transmitting medium was nitrogen. The pressure was determined using the shift of the fluorescence line of the ruby. The diffraction patterns were collected with a CCD camera, and the intensity versus 2θ patterns were obtained using the fit2d software [15]. A complete Rietveld refinement was done with the GSAS-EXPGUI package [16].

The electronic properties for the different structures were analyzed within the density functional theory (DFT) framework. We used a full-potential linearized augmented plane wave code, Wien2k [17], and GGA [18] to represent the exchange correlation potential. The positions for the ‘heavy’ elements were taken directly from the experiments while fluorine coordinates were fixed at their high symmetry positions. We did not do any relaxation or structural minimization.

In figure 1 we show the evolution with pressure of the temperature dependence of the electrical resistance of one of the two samples of CaFeAsF. The curves flatten and, above 5 GPa, show clear signs of appearance of superconductivity, as already reported [19]. The absence of percolation can be attributed to the powder nature of the sample and its sensibility to exposure to humid air during mounting, that causes insulating skins on the sample grains. We define the superconducting onset transition temperature T_c by the peak in the resistance. We also show the derivative of the resistance, with a peak that habitually signals the appearance of the antiferromagnetic ordering, T_N . While at low pressures the peak shifts to lower temperatures with pressure, at higher pressures the tendency is clearly reversed. We have also measured two samples of SrFeAsF with similar results. We plot on figure 2 the evolution of both transitions with pressure for all the samples. Differently to previously reported high-pressure measurements on 1111 materials (LaFeAsO [20], CaFeAsF [19])

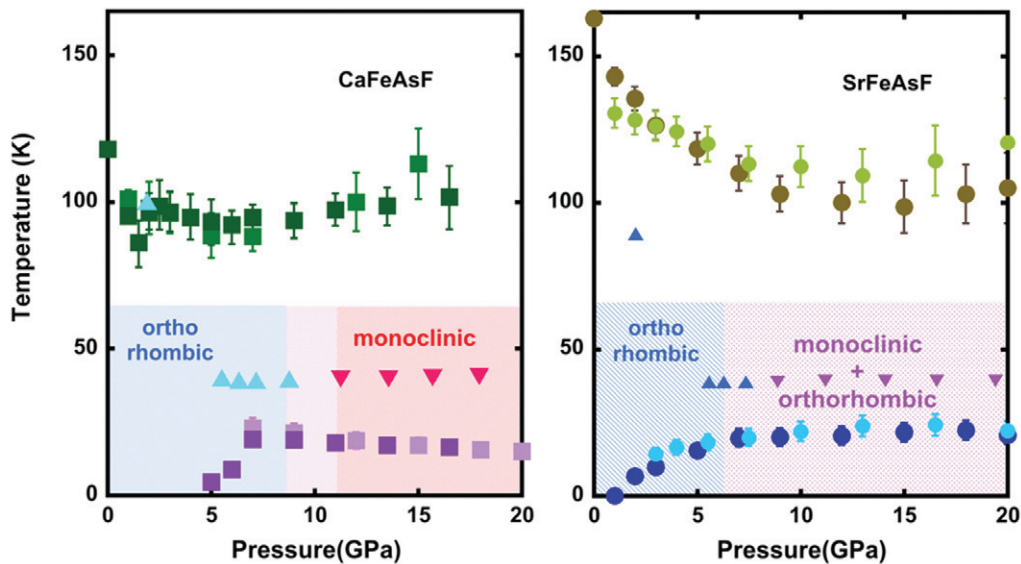


Figure 2. Left panel: pressure phase diagram for CaFeAsF, different colored squares correspond to two different samples (T_N green squares; T_C magenta squares). The triangles are taken from [21] and correspond to structural measurements that determine the nature of the distortion at the pressure and temperature of each triangle: orthorhombic (triangles) or monoclinic (inverted triangles). Superconductivity apparently only appears when the orthorhombic distortion disappears. Right panel: pressure phase diagram for SrFeAsF, different color circles correspond to two different samples (T_N green/brown circles; T_C blue circles). The triangles are taken from [21] and indicate orthorhombic (triangles) or mixed orthorhombic–monoclinic (inverted triangles). Superconductivity appears at the lowest measured pressure, there is probably coexistence of the orthorhombic and the monoclinic phase at all pressures, enabling the appearance of superconductivity in the regions where the monoclinic phase has developed (see text).

we were able to follow the evolution of the transitions for the whole pressure range, without any drop or discontinuity.

A brief description of the pressure temperature structural phase diagram of both compounds has been reported in [21]. At constant low temperature, both compounds present a transition from orthorhombic to monoclinic (shown in figure 2), with a coexistence region between both structures for SrFeAsF. On the other hand, for CaFeAsF they find a transition from the high pressure–low temperature monoclinic to the tetragonal phase at $P = 24$ GPa, $T = 200$ K, that falls within error at the extrapolation of our $T_N(P)$ curve. If we accept that the peak of the derivative is always associated with T_N , we can infer that at high pressures the antiferromagnetic state coexists with a monoclinic, not orthorhombic, phase. Concerning the development of superconductivity under pressure, it approximately coincides with the disappearance of the orthorhombic distortion for CaFeAsF, similar to what occurs in the electron-doped phase diagram. However, it now coexists with a monoclinic distortion, which has not been observed on electron doping. For the SrFeAsF compound, superconductivity is already detected for the smallest measured pressure, when the sample presumably is in the orthorhombic phase. However, according to [21], there is a large region of coexistence between the orthorhombic and the monoclinic phase, starting at approximately 6 GPa. In high-pressure x-ray measurements, a sizeable portion of the sample (>10 – 15%) must be in the monoclinic phase to be detectable, while superconductivity needs only a small percolation path. It is thus clear that superconductivity will show evidence of a very small portion of the monoclinic phase much earlier in pressure. Thus, the observed phase diagram for SrFeAsF is not in contradiction with the assumption that there is the necessity of a monoclinic phase for the

observation of superconductivity. In other words, our measurements seem to indicate that the orthorhombic phase cannot coexist with superconductivity.

The structural measurements are shown on the left panel of figure 3. At room temperature the evolution of the lattice parameters is smooth and there are no changes as have been reported for other pnictides [22, 23]. In particular, the FeAs tetrahedron is always irregular and pressure increases its irregularity. It is interesting to note that the volume of the SrFeAsF compound coincides with that of the CaFeAsF at room temperature for a pressure of 10 GPa. In fact, both compounds are electronically similar as the alkaline metal does not form bonds present at the Fermi level. It can be assumed that it is the difference in size between the Sr and Ca ions that regulates the lattice parameters, the separation between atoms and all the physical properties that depend on them. A way to test this assumption is to shift the pressure axis corresponding to the Sr compound by 10 GPa. On the right panel of figure 3 we show the effect of such a rigid shift, which verifies the assumption. The differences observed for the superconducting regions are probably due to the coexistence of the monoclinic and orthorhombic distortions in SrFeAsF, as discussed above.

Our measurements are not in complete agreement with those of Okada *et al* [19]. They measured only CaFeAsF and their phase diagram shows a brutal disappearance of T_N at 4 GPa, which we do not observe. It is followed by the sharp appearance of superconductivity at 5 GPa, more similar to what we observe. They claim that they follow T_N by the derivative of the resistance as we do, but they do not show the corresponding curves. Their work [20] on LaAsFeO shows a similar brutal disappearance of T_N at 12 GPa, but

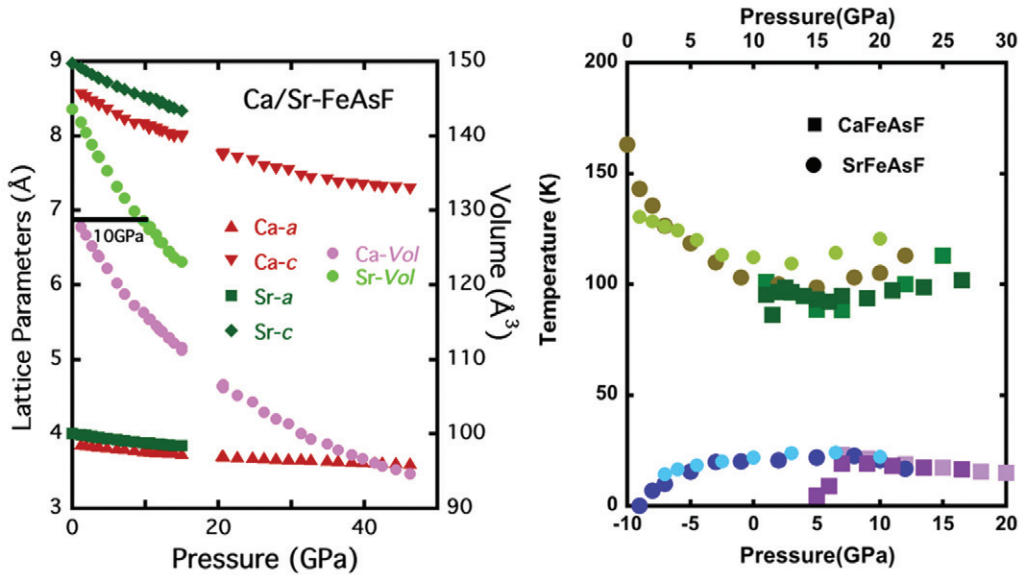


Figure 3. Left panel: evolution of the lattice parameters of Ca and Sr–FeAsF compounds with pressure. We see that 10 GPa separates both dependences, i.e. the volume of the Ca compound becomes the same as that of the Sr compound at 10 GPa. Right panel: scaling of the phase diagram for the Ca compound on the one of the Sr compound by a rigid shift of 10 GPa (upper scale, lower scale for the Sr compound). It is clear that the evolution then coincides. However, superconductivity appears suddenly for the Ca compound, which is probably due to no coexistence between the monoclinic and the orthorhombic distortions, due to a sharper transition to the presumed monoclinic phase in this compound (see text).

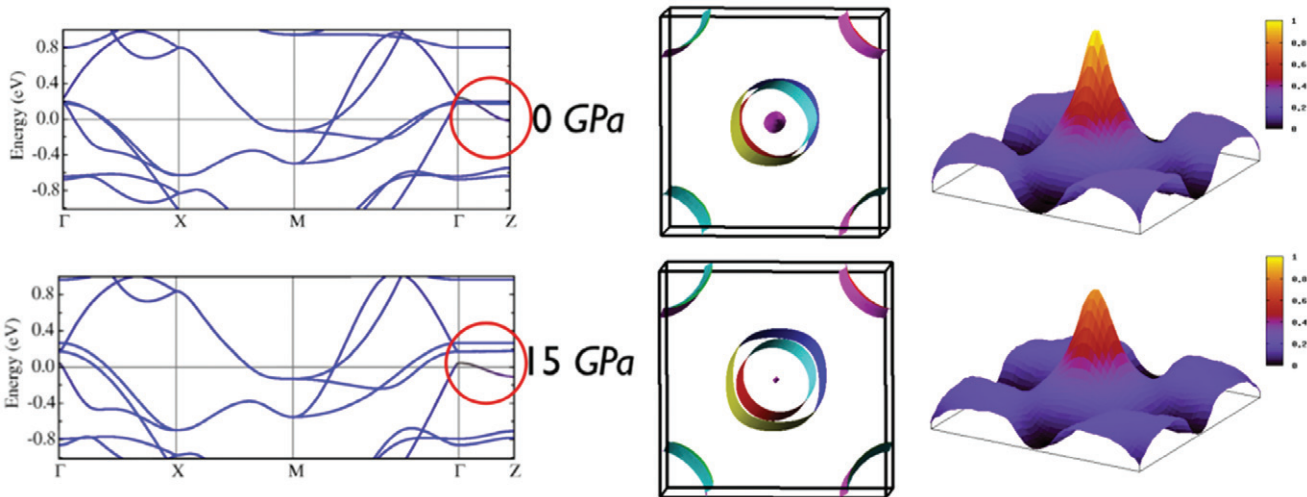


Figure 4. Effect of pressure on the electronic band structures. Left panel: band structure of CaFeAsF at two different pressures. The band in magenta between Γ and Z has a smaller Fe character (inside red circle). Central panel: as pressure increases, the hole barrel at Γ , which is due to this band, is emptied at the expense of the outer hole cylinder of full Fe character, i.e. there is an increase of hole doping of the Fe bands under pressure. Right panel: real part of the susceptibility showing that the peak remains at the same Q , although its magnitude decreases with pressure.

with superconductivity in all the pressure range, as we observe in SrFeAsF. The differences may be due to samples, measurement conditions or analysis. Obviously more work on these 1111 materials is necessary to clarify the actual phase diagram.

The phase diagrams that we have obtained are different from those reported for electron doping of 1111 compounds, suggesting that, as is the case for cuprates, pressure is equivalent to hole doping. We have performed calculations of the electronic band structure and of the Lindhard susceptibility X_q at low and high pressures from the atomic positions

determined from our structural measurements, figure 4. Considering X_q , although its magnitude decreases with pressure we do not find any change of position of the peak (as proposed in [24] for Fe_{1+x}Te) that, within the SDW scenario, should determine the magnetic ordering vector. However, it does decrease with pressure indicating that the effects of nesting also decrease. Thus, the reason why a monoclinic phase (reported in [21]) appears is not due to a change of nesting in our case and the question of the origin of the monoclinic phase remains open. Unfortunately, a determination of the magnetic structure, by e.g. neutron diffraction, would be very difficult

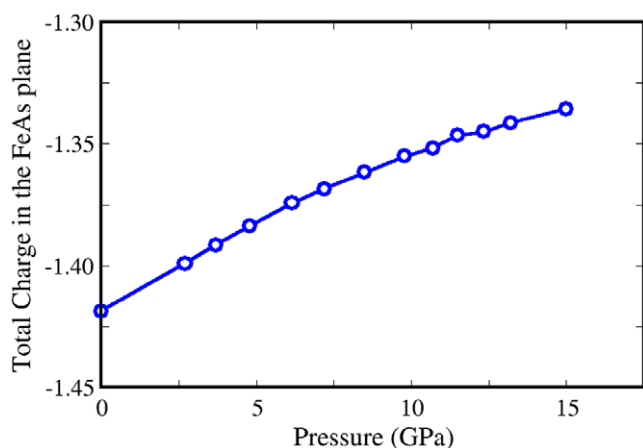


Figure 5. Total charges corresponding to the Fe–As planes as a function of the applied pressure: as pressure increases charges at these layers become less negative, so there is an effective hole doping of them. Total charges are calculated as the summation of the nuclear and the electronic Bader charges [25] corresponding to the Fe and As atoms. For this task we have used the codes *aim* (that belongs to the Wien2k package) and *critic* [27].

with the state-of-the-art experimental means. In any case, it is clear that, above the minimum of T_N , as T_N increases, T_c decreases, implying that both are based on the same parts of the Fermi surface.

Evidence for hole doping can be obtained from the evolution of the band structure and charge density at different pressures. We see in figure 4 that there is a band along ΓZ that gradually dips below the Fermi level as pressure is increased. It bonds the FeAs planes with the CaF planes. As this band absorbs electrons, the Fe–As bands responsible for antiferromagnetism and superconductivity are depleted, and the number of holes in them increases. This appears clearly from the increase in size of the hole cylinders at Γ . A similar type of phenomenon, i.e. non-Fe bands depleting Fe bands under pressure, has been reported [23] in $\text{SmFeAsO}_{0.81}\text{F}_{0.19}$. Another way to verify this effect is by doing the analysis of the Bader charges [25] corresponding to those planes. In figure 5 we plot the corresponding total charge of the Fe–As plane as a function of the applied pressure. As we can see, the Fe–As planes become less negative, i.e. doped with holes, with the application of pressure. The electrons flow to the Ca–F planes, that become more negative.

We can now compare the existing 1111 electron-doped phase diagrams to the hole-doped phase diagrams obtained by pressure. The main difference is that there is apparently coexistence of superconductivity with the antiferromagnetic state, but not with the orthorhombic distortion. It can be argued that the way in which we determine T_N is not the optimal one, but in the present state of matters it is the only available. As neutron diffraction is out of question, magnetic susceptibility measurements under pressure are necessary to confirm our results. The fact that a monoclinic to tetragonal transition has been observed at high pressures ($P = 24$ GPa, $T_{\text{mono} \rightarrow \text{tetra}} = 200$ K) and that it apparently coincides with T_N as extrapolated from our results, implies that there is a change of symmetry due to inversion of the order

of appearance of the transition temperatures, as predicted theoretically [26]. However, the relation of orthorhombicity and/or monoclinicity with superconductivity remains to be studied. Complete chemical hole doping phase diagrams are needed to clear up these doubts.

Acknowledgments

DCF gratefully acknowledges support from the Brazilian agencies CAPES and Cnpq. This work was partially supported by the project TetraFer ANR-09-BLAN-0211 of the Agence Nationale de la Recherche of France. RW is fellow of CONICET-Argentina and gratefully acknowledges partial support from CONICET (grant no. PIP 114-201101-00376) and ANPCyT (grant no. PICT-2012-0609).

References

- [1] Kamihara Y, Watanabe T, Hirano M and Hosono H 2008 *J. Am. Chem. Soc.* **130** 3296
- [2] de la Cruz C *et al* 2008 *Nature* **453** 899
- [3] Maand F and Lu Z-Y 2008 *Phys. Rev. B* **78** 033111
- [4] Huang Q *et al* 2008 *Phys. Rev. B* **78** 054529
- [5] Luetkens H *et al* 2009 *Nature Mater.* **8** 305
- [6] Zhao J *et al* 2008 *Nature Mater.* **7** 953
- [7] Rotundu C R *et al* 2009 *Phys. Rev. B* **80** 144517
- [8] Wen H-H, Mu G, Fang L, Yang H and Zhu X 2008 *Europhys. Lett.* **82** 17009
- [9] Wen H H *et al* 2009 *Physica C* **469** 894
- [10] Dagotto E 1994 *Rev. Mod. Phys.* **66** 763
- [11] Núñez-Regueiro M and Acha C 1997 *Studies of High Temperature Superconductors vol 24*, ed N V Narlikar (New York: Nova Science) p 203
- [12] Gooch M Lv, Lorenz B, Guloy A M and Chu C-W 2008 *Phys. Rev. B* **78** 180508
- [13] Zhu X, Yang H, Fang L, Mu G and Wen H-H 2008 *Supercond. Sci. Technol.* **21** 105001
- [14] Sanfilippo S *et al* 1998 *Phys. Rev. B* **61** R3800
- [15] Hammersley A P, Svensson S O, Hanfland M, Fitch A N and Hausermann D 1996 *High Pressure Res.* **14** 235
- [16] Larson A C and Von Freele 1994 *Los Alamos National Laboratory Report LUAR* pp 86–748
- [17] Toby B H 2001 *J. Appl. Crystallogr.* **34** 210
- [18] Blaha P, Schwarz K, Madsen G K H, Kvasnicka D and Luitz J 2001 *WIEN2K, An Augmented Plane Wave and Local Orbitals Program for Calculating Crystal Properties* ed K Schwarz (Vienna: University of Technology)
- [19] Perdew J P, Burke K and Ernzerhof M 1996 *Phys. Rev. Lett.* **77** 3865
- [20] Okada H *et al* 2011 *Phys. Rev. B* **81** 054507
- [21] Okada H, Igawa K, Takahashi H, Kamihara Y, Hirano M, Hosono H, Matsubayashi K and Uwatoko Y 2008 *J. Phys. Soc. Japan* **77** 113712
- [22] Mishra S K *et al* 2011 *Phys. Rev. B* **84** 224513
- [23] Garbarino G *et al* 2011 *Europhys. Lett.* **96** 57002
- [24] Garbarino G *et al* 2011 *Phys. Rev. B* **84** 024501
- [25] Han M J and Savrasov S Y 2009 *Phys. Rev. Lett.* **103** 067001
- [26] Bader R F W 1990 *Atoms in Molecules—A Quantum Theory* (Oxford: Oxford University Press)
- [27] Cano A, Civelli M, Eremin I and Paul I 2010 *Phys. Rev. B* **82** 020408
- [28] Otero-de-la-Roza A, Blanco M A, Martín Pendás A and Luaña V 2009 *Comput. Phys. Commun.* **180** 157